Optics Communications 410 (2018) 863–866

Contents lists available at ScienceDirect

Optics Communications

journal homepage: www.elsevier.com/locate/optcom

The design of atmosphere polarimetry sensing with multi-bands

Chenhao Dou [a,b], Shurong Wang [a], Zihui Zhang [a,*], Yu Huang [a], Xiaohu Yang [a], Bo Li [a]

[a] State Key Laboratory of Applied Optics, Changchun Institute of Optics, Fine Mechanics and Physics, Chinese Academy of Sciences, Changchun, Jilin 130033, China
[b] University of Chinese Academy of Sciences, Beijing 100039, China

ARTICLE INFO

Keywords:
Polarimetric imaging
Geometric optical design
Remote sensing and sensors
Lens system design

ABSTRACT

A new aerosol and cloud polarimetry sensing (ACPS) has been presented to measure four polarization components of eight specific wavelengths selected from 400 ~ 2400 nm simultaneously. The ACPS system can provide high accurate polarized intensity components of atmospheric radiance with a simple and compact structure. The ACPS structure can be regarded as a 4-f Fourier optics system. It takes Wollaston prisms as polarimeters, uses filters and slits to select the appropriate wavelength, and locates the monochromatic polarized light images on different places of focal plane. In our approach, the visible Part 1 is designed as an example and all fields MTFs of Part 1 are larger than 0.5 at detectors' Nyquist frequency 20 lp/mm.

© 2017 Published by Elsevier B.V.

1. Introduction

Both natural and anthropogenic aerosols of the atmosphere are affecting human's lives and global climate. In order to realize the role of aerosols in the global climate system, it is necessary to accurately detect the aerosol radiative forcing and retrieve the type, the contents and the distribution of the aerosol. But the remote sensing of aerosol optical thickness (AOT) and surface albedo of the earth have long been changed due to the atmosphere and surface contribution to the space-borne measurement. Therefore, the surface albedo must be removed in aerosol retrieval. The intensities measured by satellite are sensitive to both atmospheric scattering and surface albedo, while the polarized radiances are only sensitive to atmospheric scattering [1]. The polarized radiance sensitive to aerosol properties can be presented at several suitable wavelengths [2]. Therefore, a multi-band atmosphere polarimeter is required for aerosol sensing. The Glory Aerosol Polarimetry Sensor (APS) [3] is such a polarimeter and it measures the polarized radiances of 9 spectral bands. The APS optical system consists of 6 parallel telescopes (3 pairs) and 36 detectors. Each pair of telescopes covers the same 3 bands, and the intensity in four polarization directions of each band is detected through two separated assemblies. This structure is too complex to keep the system stable. In order to simplify the optical system, we designed the Aerosol and Cloud scanning Polarimetry Sensing (ACPS).

2. Concept design

The intensity and state of polarization can be described by the Stokes Vector **S** obtained from Eq. (1). In Eq. (1), I, Q, U and V are the Stocks parameters. V is negligible for solar illumination and I, Q, U can be measured just using polarizers. Therefore, we need to detect three polarization direction signals of each band at least for retrieving the Stocks Vector **S**.

$$\mathbf{S} = [I, Q, U, V]^T \tag{1}$$

To solve this problem, the Wollaston prisms are used as polarimeters in the ACPS to gather visible, near infrared and short-wave infrared light scattered from atmosphere aerosol and cloud. As shown in Fig. 1(a), the ACPS optical system contains a re-imaging structure. A beam of parallel light from the object along the Z direction (black lines in Fig. 1(a)) is collected by objective lens L0 on the slit S1 which is used to prevent the two polarization images from overlapping on the CCD. After being collimated by the collimating lens L1, the ray is spatially separated by a small divergence angle into two beams (the polarization directions of O-ray and E-ray are 0°and 90°respectively) by the Wollaston prism Wo. When the two sheared beams are re-imaged on the back focal plane of the focal lens L2, the orthogonal state images A and B are recorded by the CCD at the same time. If we slightly change the incidence angle of the beam in Fig. 1(a), the parallel light will be first imaged by the L0 on S2, and then re-imaged by the L2 on C and D. The filter LF locates behind the slits. Different positions on the surface of LF are plated different narrowband films and provide broadband spectral separation which is depicted in Fig. 1(a) and (c). Then the O-ray and E-ray signals of λ_1 and λ_2 will be imaging as line A, line B and line C, line D on CCD respectively like Fig. 1(b).

* Corresponding author.
E-mail address: ciompzhzh@sina.com (Z. Zhang).

https://doi.org/10.1016/j.optcom.2017.11.031
Received 8 October 2017; Received in revised form 6 November 2017; Accepted 11 November 2017
Available online 1 December 2017
0030-4018/© 2017 Published by Elsevier B.V.

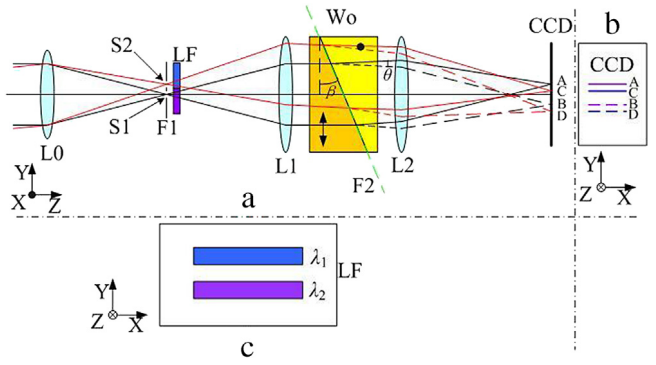

Fig. 1. (a) The schematics of ACPS. L0, objective lens; L1, collimating lens; L2, focal lens; S1, S2, slits on F1 along the X direction; Wo, Wollaston prism; F1, focal plane of L0; F2, the interface between two uniaxial crystal wedges; LF, filter. States of polarization after F2 are also shown in the picture (the real lines represent the O-ray; the broken lines represent the E-ray). The black lines are the central field, the red lines are the paraxial field. (b) The images of S1 and S2 on the CCD. (c) The schematics of the LF. λ_1, λ_2, selected wavelengths of incident light. β is the angular deviation between orthogonal pairs of polarization states. θ is the angle between the outputs of each prism pair. (For interpretation of the references to color in this figure legend, the reader is referred to the web version of this article.)

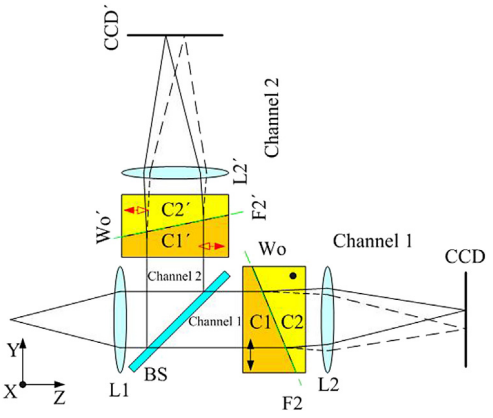

Fig. 2. The sketch map of beam splitter. BS, beam splitter. C1, C2, the two uniaxial crystal wedges of Wollaston prism Wo which resolves 0°/90° polarization components. C1', C2', the two uniaxial crystal wedges of Wollaston prism Wo' which resolves 45°/135° polarization components.

As depicted in Fig. 2, we add a beam splitter BS which is titled 45° between L1 and Wo to split collimated light into Channel 1 and Channel 2, and put another Wollaston prism Wo' which has been rotated by 45° anticlockwise in YZ plane to resolve the 45°/135° components. Another focal lens L2' focalize the Channel 2 light on the CCD'. In this manner, the four polarization atmosphere radiation for each spectral band could be detected by ACPS at one time.

3. Lens design result

There are eight spectral bands (443, 555, 670, 865, 910, 1378, 1605 and 2210 nm) selected for the ACPS instrument [4]. Six of the eight spectral bands (443, 555, 670, 865, 1605 and 2210 nm) are consistent with an optimized aerosol retrieval strategy because they take advantage of several natural circumstances while the remaining two bands (910 and 1378 nm) are used to measure water vapor and to screen for cirrus clouds respectively [5].

Due to the limit of the transmittance of optical materials and the dramatic change of the solar reflective spectrum from 400 to 2400 nm which cannot be measured by just one kind of detector, the ACPS optical structure is divided into three relatively independent parts which are designed in accordance with the principle of Figs. 1 and 2. Part 1 has four

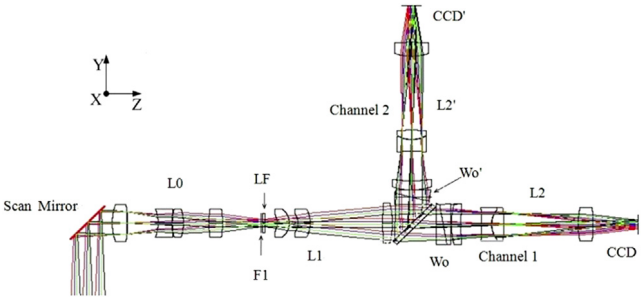

Fig. 3. The layout of Part 1 of ACPS. L0, L1, L2, L2', F1, LF, Wo, Wo', CCD and CCD' have been introduced in Fig. 1 and Fig. 2. The X direction is the orbit direction.

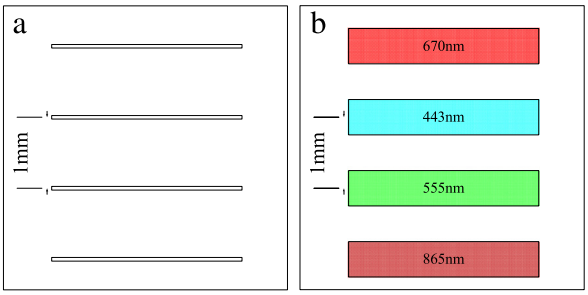

Fig. 4. The plane distributing plot of F1 and LF (a) F1; (b) LF. F1 and LF has been introduced in Fig. 1.

Table 1
Performance parameters of Part 1.

Parameter	Requirement
Spectral bands	443. 555, 670, 865 nm
FWHM	20 nm
IFOV	±2.4° (Cross-track) ±2.08° (Along-track)
Field of view	±36°
Focal length	37 mm
F number	3.7

narrow bands in visible region (420–880 nm), and part 2 and 3 works respectively in the near infrared region (880–1400 nm) and short-wave infrared region (1550–2260 nm). Now, we design Part 1 as an example which is shown in Fig. 3.

The Part 1 of ACPS employs two Wollaston prisms and two area array CCDs. In order to satisfy the requirements in detecting the aerosol, we put a scanning mirror in front of the camera. By scanning, the incident light can converge at different films of LF and change into monochromatic light of specific wavelengths. But scanning may also result in a little time-delay between different wavelengths. The performance parameters of the proposed Part 1 are listed in Table 1. We can regard Part 1 as a 4-f Fourier optics system. Therefore, the lens L0, L1, L2 are all $f/37$ mm, F#3.7 camera objectives. We designed the prisms Wo and Wo' of Part 1, and the $15 \times 15 \times 8$ mm optic was custom-fabricate from calcite. In order to minimize lateral chromatic aberration effects in the polarimeter, the incident angles are designed relatively small. When the incident angle of Wollaston prism is small, the change of splitting angle is slight [6]. For small angles, the θ in Fig. 1 equals to $\beta \cdot (n_o - n_e)$. The distance α between the O-ray and E-ray of one wavelength on the CCD is equal to $f_2 \cdot \tan\theta$, where f_2 is the focus of L2 and L2' in Fig. 3. When the birefringence material is calcite, the values of $\alpha = 0.5$ mm, $\theta = 0.78°$ and $\beta = 5°$ are chosen to make sure that the sufficient polarization rays are separated and imaged on the imagers [7].

Fig. 4(a) shows the distribution of the slits (the size of slits are 0.7×0.05 mm) on F1. Fig. 4(b) describes the plane distributing plot

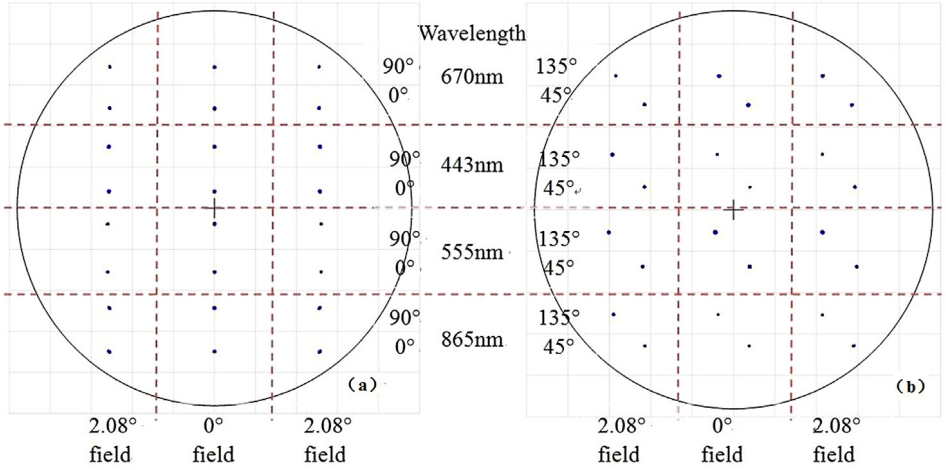

Fig. 5. Spot diagram for optic system (a) Channel 1; (b) Channel 2. States of polarization of each wavelength are also shown in inset.

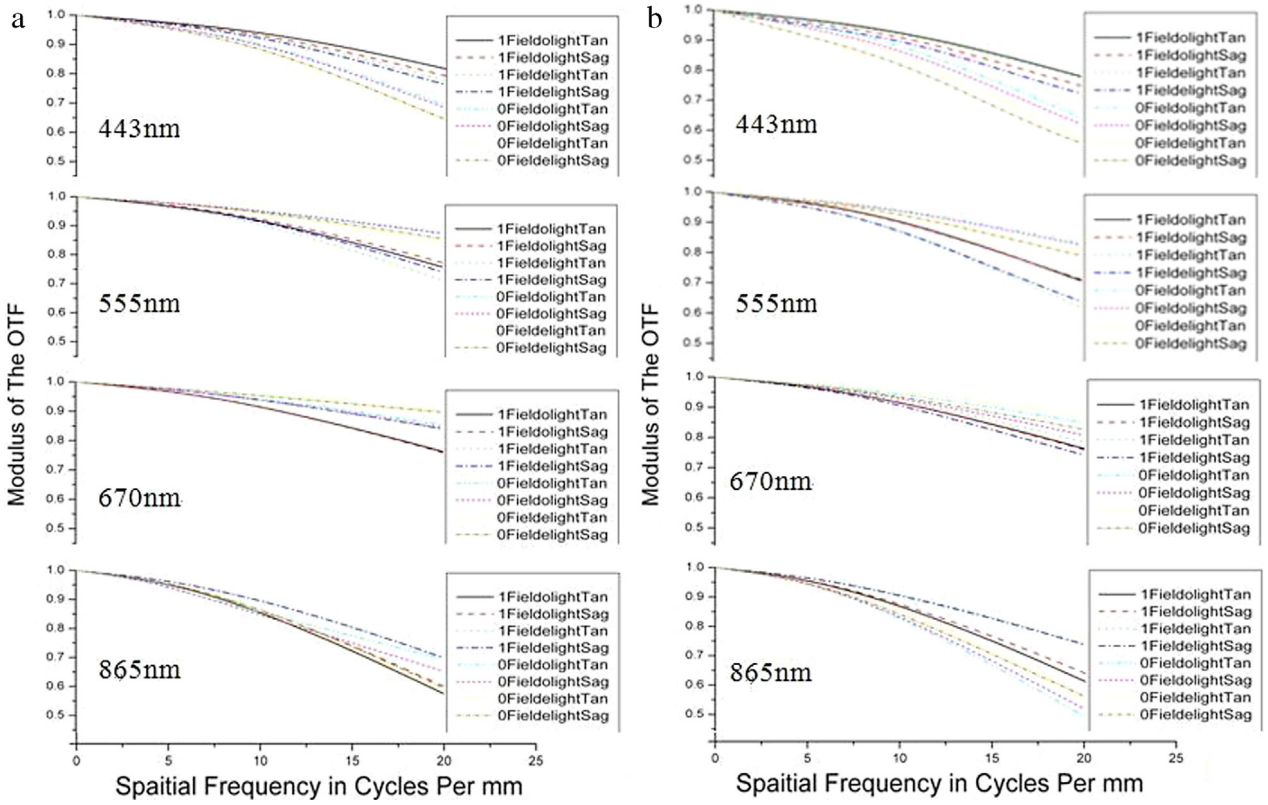

Fig. 6. MTF curves for the optic system (a) Channel 1; (b) Channel 2.

of films (the size of films are 1×0.05 mm) on LF. As shown in Fig. 4(b), in order to reduce axial chromatic aberration, we put the films of longer wavelengths on the edge of LF.

The optical systems of L0 and L1 in Fig. 3 consist of three or four lenses with a telephoto telecentric structure in the image space to guarantee that the beams are perpendicular to the filter and the lens are small in size. Through optimizing design, the RMS of spot diagrams of Channel 1 and Channel 2 in Part 1 are all smaller than 13.5 μm, and their distribution and polarization states are shown in Fig. 5(a) and (b) respectively. Fig. 6 plots the modulation transfer functions (MTFs), and the MTFs of all fields are above 0.5 at detectors' Nyquist frequency 20 lp/mm.

4. Conclusion

In conclusion, a secondary imaging atmosphere polarimeter design concept has been presented. The design result of ACPS's visible part has been demonstrated as an example. The near infrared and short-wave infrared parts are identical with the visible part in principle and structure, and they are just different in working wavelengths. Each part of the ACPS which contains no moving polarization elements can characterize the four polarizations for each wavelength at one time by using one filter, two Wollaston prisms and two detectors. The ACPS is a simple and accurate multi-band polarization measuring system. It is designed mainly to measure aerosol content and cloud coverage in

atmosphere on moving remote-sensing platforms. Besides, this structure may be used in other atmosphere polarimetry fields, such as atmosphere dust [8], cloud information [9], water vapor [10] and so on. The only defect of the ACPS system is that there is a little time-delay between different wavelengths which can be modified by suitable algorithms. And the key technology aporia in ACPS's development is the production of filter. We can combine several filters with different films together to replace the LF in Fig. 3 to solve this problem. Compared with Glory APS, the optical system of ACPS is more simple and compact. Because the ACPS only takes 4 array detectors, its electronics module is smaller.

Acknowledgment

This work was supported by the National Natural Science Foundation of China, No. 11573025.

References

[1] M. Duan, D. Lv, Chin. J. Atomsphere. Sci. 31 (2007) 757.
[2] K.N. Liou, An Introduction to Atmospheric Radiation, second ed., Academic Press, 2002, p. 336.
[3] S. Persh, Y.J. Shaham, O. Benami, B. Cairns, M.I. Mishchenko, J.D. Hein, B.A. Fafaul, SPIE 7807 (2010) 780703.
[4] J.D. Perreault, Opt. Lett. 38 (2013) 3874.
[5] R.J. Peralta, C. Nardell, B. Cairns, E.E. Russell, L.D. Travis, M.I. Mishchenko, B.A. Fafaul, R.J. Hooker, SPIE 6786 (2007) 67865L.
[6] O. Masihzadeh, P. Schlup, R.A. Bartels, Opt. Express 15 (2007) 18026.
[7] H. Yao, G. Li, H. Peng, G. Wang, L. Kong, J. Qufu. Normal. Univ. 34 (2008) 51.
[8] N. Sugimoto, T. Nishizawa, A. Shimizu, Y. Jin, Light, Energy and the Environment Congress. EW2A.1.pdf, 2016.
[9] A. Barta, G. Horváth, et al., Appl. Opt. 54 (2015) 1065.
[10] S. Wu, X. Song, et al., Opt. Express 23 (2015) 33870.